Reduced Gene Dosage of Histone H4 Prevents CENP-A Mislocalization in Budding Yeast

Jessica R. Eisenstatt*, Kentaro Ohkuni*, Olivia Preston*, Wei-Chun Au*, Michael Costanzo[†, ‡], Charles Boone[†, ‡], and Munira A. Basrai*

*Genetics Branch, Center for Cancer Research, National Cancer Institute, National Institutes of Health, Bethesda, Maryland 20894, [†]Department of Molecular Genetics, University of Toronto and [‡]Donnelly Centre for Cellular and Biomolecular Research, Toronto, Ontario M5S 3E1, Canada

Running Title (35 characters): H4 Promotes CENP-A Mislocalization

Keywords (up to 5): Centromere, CENP-A, Histone H4, Psh1

Corresponding Author: Munira A. Basrai, Genetics Branch, National Cancer Institute, National Institutes of Health, 41 Medlars Drive, Rm B624, Bethesda, MD 20892. E-mail: basraim@mail.nih.gov Phone: 240-760-6746

ABSTRACT

Mislocalization of the centromeric histone H3 variant (Cse4 in budding yeast, CID in flies, CENP-A in humans) contributes to chromosomal instability (CIN) in yeast, fly, and human cells. Overexpression and mislocalization of CENP-A has been observed in several cancers. However, the mechanisms that contribute to the mislocalization of CENP-A are not fully understood. In this study, we used budding yeast to identify genes that facilitate the mislocalization of Cse4 to non-centromeric regions. Previous studies have shown that E3 ligases (Psh1, Slx5, Cdc4) and factors such as Doa1, Hir2, and Cdc7 regulate proteolysis of Cse4 and prevent its mislocalization. Overexpressed Cse4 (*GALCSE4*) is highly stable and causes synthetic dosage lethality (SDL) in *psh1Δ*, *slx5Δ*, *doa1Δ*, *hir2Δ*, *cdc4-1*, and *cdc7-4* strains. We used a genome-wide screen to identify suppressors of the *psh1Δ GALCSE4* SDL. Deletions of histone H4 alleles (*HHF1* or *HHF2*) were among the top suppressors of *psh1Δ GALCSE4* SDL. Here we show that reduced gene dosage of *H4* prevents mislocalization of Cse4 and promotes faster degradation of Cse4 in a *psh1Δ GALCSE4* strain. Deletion of either *HHF1* or *HHF2* also suppresses the *GALCSE4* SDL in *slx5Δ*, *doa1Δ*, *hir2Δ*, *cdc4-1*, and *cdc7-4* strains. Suppression of *psh1Δ GALCSE4* SDL by *hhf1-20*, which is defective for interaction with Cse4, suggests that defects in the Cse4-H4 interaction prevents mislocalization of Cse4. In summary, our genome-wide screen identified genes that contribute to Cse4 mislocalization and we show how reduced dosage of histone H4-encoding genes prevents mislocalization of Cse4 into non-centromeric regions.

INTRODUCTION

Centromeres are specialized chromosome loci that are essential for faithful chromosome segregation during mitosis and meiosis. The kinetochore (centromeric DNA and associated proteins) provides an attachment site for microtubules for segregation of sister chromatids during cell division (ALLSHIRE AND KARPEN 2008; VERDAASDONK AND BLOOM 2011; BURRACK AND BERMAN 2012; CHOY *et al.* 2012; MADDOX *et al.* 2012; MCKINLEY AND CHEESEMAN 2016). Despite the wide divergence of centromere DNA sequence, establishment of centromeric chromatin is highly regulated by epigenetic mechanisms where incorporation of the essential and evolutionarily conserved centromeric histone H3 variant CENP-A (Cse4 in *Saccharomyces cerevisiae*, Cnp1 in *Schizosaccharomyces pombe*, CID in *Drosophila melanogaster*, and CENP-A in mammals) serves to nucleate kinetochore assembly (KITAGAWA AND HIETER 2001; BIGGINS 2013; MCKINLEY AND CHEESEMAN 2016). Cellular levels of CENP-A are stringently regulated and overexpression of CENP-A leads to its mislocalization to non-centromeric chromatin and contributes to aneuploidy in yeast, flies, and humans (COLLINS *et al.* 2004; HEUN *et al.* 2006; MORENO-MORENO *et al.* 2006; AU *et al.* 2008; MISHRA *et al.* 2011; LACOSTE *et al.* 2014; ATHWAL *et al.* 2015; SHRESTHA *et al.* 2017). Overexpression and mislocalization of CENP-A is observed in many cancers and is proposed to promote tumorigenesis (TOMONAGA *et al.* 2003; AMATO *et al.* 2009; LI *et al.* 2011; MCGOVERN *et al.* 2012; SUN *et al.* 2016). Thus, molecular mechanisms that promote and prevent mislocalization of CENP-A is an area of active investigation.

In budding yeast, post-translational modifications (PTMs) of Cse4, such as ubiquitination, sumoylation, and isomerization, are important for regulating steady-state levels of Cse4 and preventing its mislocalization to non-centromeric regions, thereby maintaining

chromosome stability (COLLINS *et al.* 2004; HEWAWASAM *et al.* 2010; RANJITKAR *et al.* 2010; OHKUNI *et al.* 2014; OHKUNI *et al.* 2016; CHENG *et al.* 2017; AU *et al.* 2020). Ubiquitin-mediated proteolysis of Cse4 by E3 ubiquitin ligases such as Psh1 (HEWAWASAM *et al.* 2010; RANJITKAR *et al.* 2010), Slx5 (OHKUNI *et al.* 2016), $SCF^{Met30/Cdc4}$ (AU *et al.* 2020), SCF^{Rcy1} (CHENG *et al.* 2016), and Ubr1 (CHENG *et al.* 2017) and proline isomerase Fpr3 (OHKUNI *et al.* 2014) regulate the cellular levels of Cse4. Psh1-mediated proteolysis of Cse4 has been well characterized and has been shown to be regulated by the FACT (Facilitates Chromatin Transcription/Transactions) complex (DEYTER AND BIGGINS 2014), CK2 (Casein Kinase 2) (HEWAWASAM *et al.* 2014), HIR (HIstone Regulation) histone chaperone complex (CIFTCI-YILMAZ *et al.* 2018), and DDK (Dbf4-Dependent Kinase) complex (EISENSTATT *et al.* 2020). In general, mutation or deletion of these factors that prevent Cse4 mislocalization show synthetic dosage lethality (SDL) when Cse4 is overexpressed from a galactose-inducible promoter (*GALCSE4*).

The evolutionarily conserved CENP-A specific histone chaperones (Scm3 in *S. cerevisiae* and *S. pombe*, CAL1 in *D. melanogaster*, Holliday Junction Recognition Protein HJURP in humans) mediate the centromeric localization of CENP-A (CAMAHORT *et al.* 2007; MIZUGUCHI *et al.* 2007; STOLER *et al.* 2007; FOLTZ *et al.* 2009; PIDOUX *et al.* 2009; WILLIAMS *et al.* 2009; SHUAIB *et al.* 2010; CHEN *et al.* 2014). In budding yeast, chaperones other than Scm3 can facilitate the deposition of overexpressed CENP-A when the balance of H3 and CENP-A is altered. For example, the Chromatin Assembly Factor 1 (CAF-1), an evolutionarily conserved replication-coupled histone H3/H4 chaperone, promotes localization of overexpressed Cse4 to centromeres when Scm3 is depleted in *S. cerevisiae* (HEWAWASAM et al. 2018). The CAF-1 orthologues Mis16 in *S. pombe* and RbAp46/48 in humans and *D. melanogaster* also contribute to centromeric localization of CENP-A (FUJITA *et al.* 2007; PIDOUX *et al.* 2009; WILLIAMS *et al.*

2009; BOLTENGAGEN *et al.* 2016). In contrast to CENP-A deposition at centromeric regions, mechanisms that facilitate the mislocalization of CENP-A to non-centromeric regions have not been fully explored. Studies from our laboratory and those of others show that the transcription-coupled histone H3/H4 chaperone DAXX/ATRX promotes mislocalization of CENP-A to non-centromeric regions in human cells (LACOSTE *et al.* 2014; SHRESTHA *et al.* 2017). In budding yeast, CAF-1 contributes to the mislocalization of Cse4 to non-centromeric regions (HEWAWASAM *et al.* 2018). We have recently shown that sumoylation of the C-terminus of Cse4 facilitates its interaction with CAF-1 and this promotes the deposition of Cse4 to non-centromeric regions (OHKUNI *et al.* 2020). Notably, *psh1*Δ *cac2*Δ with *GALCSE4* and *psh1*Δ with *GALcse4*$^{K215/216R/A}$ do not exhibit SDL due to reduced mislocalization of Cse4 (HEWAWASAM *et al.* 2018; OHKUNI *et al.* 2020).

Defining the mechanisms that facilitate the mislocalization of Cse4 to non-centromeric regions is essential for understanding chromosomal instability (CIN). We performed a genome-wide screen using a synthetic genetic array (SGA) to identify genes that promote Cse4 mislocalization. We took advantage of the SDL of a *psh1⊿ GALCSE4* strain (HEWAWASAM *et al.* 2010; RANJITKAR *et al.* 2010; AU *et al.* 2013) to identify suppressors of the SDL phenotype. An SGA analysis was performed by combining mutants of essential genes and deletion of non-essential genes with *psh1*Δ *GALCSE4*. The screen identified mutations or deletions of genes encoding regulators of chromatin remodeling, RNA transcription/processing, nucleosome occupancy, ubiquitination, and histone H4. Deletion of the two alleles that encode histone H4 (*HHF1* or *HHF2*) were among the most prominent suppressors of the *psh1⊿ GALCSE4* SDL.

In this study, we focused on understanding how reduced gene dosage of *H4* suppresses the SDL of a *psh1⊿ GALCSE4* strain. The budding yeast genome possesses two gene pairs which

encode identical H3 and H4 proteins (*HHT1/HHF1* and *HHT2/HHF2*) and two gene pairs which encode identical H2A and H2B proteins (*HTA1/HTB1* and *HTA2/HTB2*). We show that deletion of either allele of histone H4 (*HHT1/hhf1*Δ or *HHT2/hhf2*Δ), but not histone H3 (*hht1*Δ*/HHF1* or *hht2*Δ*/HHF2*) or histone H2A (*hta1*Δ*/HTB1* or *hta2*Δ*/HTB2*), suppresses the SDL phenotype of a *psh1Δ GALCSE4* strain. We determined that deletion of *HHF1* or *HHF2* suppresses the mislocalization of Cse4 to non-centromeric regions in a *psh1Δ* strain and a *hhf2Δ psh1Δ* strain displays faster degradation of Cse4. Deletion of *HHF1* or *HHF2* also suppresses the *GALCSE4* SDL in *slx5Δ*, *doa1Δ*, *hir2Δ*, *cdc4-1*, and *cdc7-4* strains. Moreover, *hhf1-20*, which has mutations in the H4 histone fold domain and is defective for interaction with Cse4, (SMITH *et al*. 1996; GLOWCZEWSKI *et al*. 2000) suppresses the *psh1Δ GALCSE4* SDL, suggesting that the Cse4-H4 interaction is required for association of Cse4 with chromatin. In summary, our genome-wide suppressor screen allowed us to identify genes that contribute to Cse4 mislocalization and to define a role for the gene dosage of *H4* in facilitating the mislocalization of Cse4 into non-centromeric regions.

MATERIALS AND METHODS

Strains and Plasmids

Yeast strains used in this study are described in Table S2 and plasmids in Table S3. Yeast strains were grown in rich media (1% yeast extract, 2% bacto-peptone, 2% glucose) or synthetic medium with glucose or raffinose and galactose (2% final concentration each) and supplements to allow for selection of the indicated plasmids. Double mutant strains were generated by mating wild type or *psh1Δ* strains with empty vector or a plasmid containing *GAL1-6His-3HA-CSE4* to mutant strains on rich medium at room temperature for six hours followed by selection of diploid cells on medium selective for the plasmid and appropriate resistance markers. Diploids were sporulated for 5 days at 23°C and plated on selective medium without uracil, histidine, or arginine and with canavanine, clonNAT, and G418 to select for MATa double mutants. The synthetic genetic array (SGA) was performed as previously described (COSTANZO *et al.* 2016).

Growth assays

Growth assays were performed as previously described (EISENSTATT *et al.* 2020). Wild type and mutant strains were grown on medium selective for the plasmid, suspended in water to a concentration with an optical density of 1 measured at a wavelength of 600 nm (OD_{600}, approximately 1.0 X 10^7 cells per ml), and plated in five-fold serial dilutions starting with 1 OD_{600} on synthetic growth medium containing glucose or galactose and raffinose (2% final concentration each) selecting for the plasmid. Strains were grown at the indicated temperatures for 3-5 days.

Protein stability assays

Protein stability assays were performed as previously described (AU *et al.* 2008). Briefly, logarithmically growing wild type and mutant cells were grown for four hours in media selective for the plasmid containing galactose/raffinose (2% final concentration each) at 30°C followed by addition of cycloheximide (CHX, 10 µg/ml) and glucose (2% final concentration). Protein

extracts were prepared from cells collected 0, 30, 60, 90, and 120 minutes after CHX addition with the TCA method as described previously (KASTENMAYER *et al.* 2006). Equal amount of protein as determined by the Bio-Rad DC™ Protein Assay were analyzed by Western blot. Proteins were separated by SDS-PAGE on 4-12% Bis-TRIS SDS-polyacrylamide gels (Novex, NP0322BOX) and analysis was done against primary antibodies α-HA (1:1000, Roche, 12CA5) or α-Tub2 (1:4500, custom made for Basrai Laboratory) in TBST containing 5% (w/v) dried skim milk. HRP-conjugated sheep α-mouse IgG (Amersham Biosciences, NA931V) and HRP-conjugated donkey α-rabbit IgG (Amersham Biosciences, NA934V) were used as secondary antibodies. Stability of the Cse4 protein relative to the Tub2 loading control was measured as the percent remaining as determined with the Image Lab Software (BioRad).

Ubiquitination Pull-down Assay

Levels of ubiquitinated Cse4 were determined with ubiquitin pull-down assays as described previously (AU *et al.* 2013) with modifications. Cells were grown to logarithmic phase, induced in galactose-containing medium for 3 hours at 30^{o}C and pelleted. The cell pellet was resuspended in lysis buffer (20 mM Na_2HPO_4, 20 mM NAH_2PO_4, 50 mM NaF, 5 mM tetra-sodium pyrophosphate, 10 mM beta-glycerolphosphate, 2 mM EDTA, 1 mM DTT, 1% NP-40, 5 mM N-Ethylmaleimide, 1 mM PMSF, and protease inhibitor cocktail (Sigma, catalogue # P8215)) and equal volume of glass beads (lysing matrix C, MP Biomedicals). Cell lysates were generated by homogenizing cells with a FastPrep-24 5G homogenizer (MP Biomedicals) and a fraction of the lysate was aliquoted for input. An equal concentration of lysates from wild type and mutant strains were incubated with tandem ubiquitin binding entities (Agarose-TUBE1, Life Sensors, Inc., catalogue # UM401) overnight at 4°C. Proteins bound to the beads were washed three times with TBS-T at room temperature and eluted in 2 x Laemmli buffer at 100°C for 10 minutes. The eluted protein was resolved on a 4-12% Bis-Tris gel (Novex, NP0322BOX) and ubiquitinated Cse4 was detected by Western blot using anti-HA antibody (Roche Inc., 12CA5). Levels of ubiquitinated Cse4 relative to the non-modified Cse4 in the input were quantified using

171 software provided by the Syngene imaging system. The percentage of ubiquitinated Cse4 levels
172 is set to 100% in the wild type strain.

173 **ChIP-qPCR**

174 Chromatin immunoprecipitations were performed with two biological replicates per
175 strain as previously described (COLE *et al.* 2014; CHEREJI *et al.* 2017; EISENSTATT *et al.* 2020)
176 with modifications. Logarithmic phase cultures were grown in raffinose/galactose (2% final
177 concentration each) media for 4 hours and were treated with formaldehyde (1% final
178 concentration) for 20 minutes at 30°C followed by the addition of 2.5 M glycine for 10 minutes
179 at 30°C. Cell pellets were washed twice with 1 X PBS and resuspended in 2 mL FA Lysis Buffer
180 (1 mM EDTA pH8.0, 50 mM HEPES-KOH pH7.5, 140 mM NaCl, 0.1% sodium deoxycholate,
181 1% Triton X-100) with 1 x protease inhibitors (Sigma) and 1 mM PMSF (final concentration).
182 The cell suspension was split into four screw top tubes with glass beads (0.4-0.65 mm diameter)
183 and lysed in a FastPrep-24 5G (MP Biosciences) for 40 seconds three times, allowed to rest on
184 ice for 5 minutes, and lysed two final times for 40 seconds each. The cell lysate was collected,
185 and the chromatin pellet was washed in FA Lysis Buffer twice. Each pellet was resuspended in
186 600 µl of FA Lysis Buffer and combined into one 5 ml tube. The chromatin suspension was
187 sonicated with a Branson digital sonifer 24 times at 20% amplitude with a repeated 15 seconds
188 on/off cycle. After 3 minutes of centrifugation (13000 rpm, 4ºC), the supernatant was transferred
189 to another tube. Input sample was removed (5%) and the average size of the DNA was analyzed.
190 The remaining lysate was incubated with anti-HA-agarose beads (Sigma, A2095) overnight at
191 4°C. The beads were washed in 1 ml FA, FA-HS (500 mM NaCl), RIPA, and TE buffers for five
192 minutes on a rotor two times each. The beads were suspended in ChIP Elution Buffer (25 mM
193 Tris-HCl pH7.6, 100 mMNaCl, 0.5% SDS) and incubated at 65°C overnight. The beads were
194 treated with proteinase K (0.5 mg/ml) and incubated at 55°C for four hours followed by

Phenol/Chloroform extraction and ethanol precipitation. The DNA pellet was resuspended in a total of 50 µl sterile water. Samples were analyzed by quantitative PCR (qPCR) performed with the 7500 Fast Real Time PCR System with Fast SYBR Green Master Mix (Applied Biosystems). qPCR conditions used: 95°C for 20 sec; 40 cycles of 95°C for 3 sec, 60° for 30 sec. Primers used are listed in Table S4.

Data availability

Strains and plasmids are available upon request. Supporting figures S1-S4 are available as JPG files. Supporting Table S1 is an Excel file that describes mutations that suppress the *psh1Δ GALCSE4* SDL, the gene systematic name, the gene name, the functional category, growth and colony scores, and validation information if applicable. File S1 contains Tables S2, S3, and S4 which describe the yeast strains, plasmids, and primers used in this study, respectively.

RESULTS

A genome-wide screen identified suppressors of the SDL phenotype of a *psh1Δ GALCSE4* strain

Identifying pathways that facilitate the deposition of Cse4 to non-centromeric regions will provide insight into the mechanisms that promote chromosomal instability (CIN). Deletion of *PSH1*, which regulates ubiquitin-mediated proteolysis of Cse4, results in synthetic dosage lethality (SDL) when Cse4 is overexpressed (HEWAWASAM *et al.* 2010; RANJITKAR *et al.* 2010). We reasoned that strains with deletions or mutations of factors that promote Cse4 mislocalization would rescue the SDL of a *psh1Δ* strain overexpressing Cse4. Therefore, we generated a *psh1Δ* query strain with *6His-3HA-CSE4* on a galactose-inducible plasmid (*GALCSE4*) and mated it to arrays of 3,827 non-essential gene deletion strains and of 786 conditional mutant alleles, encoding 560 essential genes, and 186 non-essential genes for internal controls (COSTANZO *et al.* 2016). Growth of the haploid meiotic progeny plated in quadruplicate was visually scored on glucose-and galactose-containing media grown at 30°C for non-essential and 26°C for essential gene mutant strains (Figure 1A). Highlighted in the figure are all four replicates of deletion of histone H4 (*hhf1Δ*) and Hap3 (*hap3Δ*) showing better growth on galactose media compared to the control strains along the perimeter and other deletion strains on the plate (Figure 1B, bottom and top square, respectively). Strains that suppress the *psh1Δ GALCSE4* SDL on galactose-containing media were given a growth score of one (low suppression) to four (high suppression) (Table S1). The number of replicates within the quadruplicate that displayed the same growth were given a colony score of one (one out of four replicates) to four (all four replicates). We identified ninety-four deletion and mutant alleles encoding ninety-two genes that suppressed the

psh1Δ GALCSE4 SDL and the majority (81%) of quadruplicates had all four colonies displaying the same level of suppression, indicated by a colony score of four (Table S1).

Of the ninety-four alleles, we selected thirty-eight candidate mutants (fourteen non-essential deletion strains and twenty-four conditional mutants) to confirm the suppression of *psh1Δ GALCSE4* SDL (Table 1). These candidates displayed a growth score of three or four where most of the replicates displayed high suppression and represent pathways involved in RNA processing and cleavage, DNA repair, chromatin remodeling, histone modifications, and DNA replication (Table 1). Secondary validation of the SDL suppressors was done by independently generating double mutant strains of *psh1Δ GALCSE4* with candidate mutants. Growth assays were performed on media selective for the *GALCSE4* plasmid and containing either glucose or raffinose and galactose. We used a *hir2Δ psh1Δ* strain as a negative control because *hir2Δ psh1Δ GALCSE4* strains display SDL (CIFTCI-YILMAZ *et al.* 2018). Of the thirty-eight strains tested, twenty-nine showed almost complete suppression, five strains showed a partial suppression, and four did not suppress the SDL on galactose media (Tables 1 and S1 and Figures S1A and S1B). We further tested a subset of the thirty-eight genes to confirm overexpression of *GAL1-6His-3HA-CSE4* and found that strains with mutations in genes involved in RNA processing and transcription do not show galactose-induced expression of *GAL1-6His-3HA-CSE4* (Table S1 and Figure S1C), indicating that these are false positive hits. Taken together, secondary validation confirmed that 89% of the candidate mutants tested suppressed the *psh1Δ GALCSE4* SDL.

Our screen identified deletion and mutant alleles corresponding to three components of the INO80 chromatin remodeling complex, Ies2, Arp8, and Act1 (POCH AND WINSOR 1997; SHEN *et al.* 2000; SHEN *et al.* 2003; TOSI *et al.* 2013). Secondary validation assays showed that

ies2Δ and *act1-132* do not suppress the SDL of the *psh1Δ GALCSE4* strain (Figures S1A and S1B). In contrast, *arp8Δ* did suppress the *psh1Δ GALCSE4* SDL (Figures S1A and S2A) however, the *arp8Δ* strain displayed polyploidy when analyzed by Fluorescent Activated Cell Sorting (FACS) (Figure S2B), consequently we did not pursue it further.

Deletion of histone H4 alleles suppresses the SDL of a *psh1Δ GALCSE4* strain

Two nonallelic loci, *HHT1/HHF1* and *HHT2/HHF2,* encode identical H3 and H4 proteins in budding yeast. The screen identified the deletion of either one of the histone H4 alleles, *HHT1/hhf1*Δ (*hhf1Δ*) or *HHT2/hhf2*Δ (*hhf2Δ*), as among the most prominent suppressors of the *psh1Δ GALCSE4* SDL. A role for the dosage of histone H4-encoding genes in mislocalization of Cse4 has not yet been reported. We confirmed that the *hhf1Δ* and *hhf2Δ* strains do not exhibit defects in ploidy or cell cycle by FACS analysis (Figure S3). Growth assays were done to confirm the suppression of SDL by deleting *HHF1* or *HHF2* in *psh1Δ GALCSE4* strains and *psh1Δ* strains with empty vector as controls. Our results showed that *psh1Δ hhf1Δ* and *psh1Δ hhf2Δ* strains plated on galactose media rescued the growth defect of the *psh1Δ GALCSE4* strain (Figure 2A). We determined that the phenotype was linked to deletion of the H4 alleles because transformation of a plasmid with the respective wild type histone H4 gene into the *psh1Δ hhf1Δ* or *psh1Δ hhf2Δ* strains restored the SDL observed in the *psh1Δ GALCSE4* strain (Figure 2B).

We next sought to investigate if deletion of a single allele for either histone H3 or H2A genes could suppress the SDL of a *psh1Δ* strain. Note that the two nonallelic loci, *HTA1/HTB1* and *HTA2/HTB2*, encode almost identical H2A and H2B proteins. Deletion of *HTA1* (*hta1Δ/HTB1*), *HTA2* (*hta2Δ/HTB2*), *HHT1* (*hht1Δ/HHF1*), or *HHT2* (*hht2Δ/HHF2*) did not suppress the SDL of a *psh1Δ GALCSE4* strain in growth assays (Figures 2C and 2D and Table

2). Based on these results we conclude that the suppression of *psh1Δ GALCSE4* SDL is specific to the reduced gene dosage of *H4*.

Reduced gene dosage of *H4* suppresses the SDL of *slx5Δ, doa1Δ, hir2Δ, cdc4-1,* and *cdc7-4 GALCSE4* strains

To determine if the SDL suppression by reduced *H4* gene dosage is limited to the *psh1Δ GALCSE4* strain, we deleted *HHF1* or *HHF2* in deletion or mutant strains encoding Slx5, Doa1, Hir2, Cdc4, and Cdc7 as deletion or mutation of these factors show SDL with *GALCSE4* and mislocalization of transiently overexpressed Cse4 (AU *et al.* 2013; OHKUNI *et al.* 2016; CIFTCI-YILMAZ *et al.* 2018; AU *et al.* 2020; EISENSTATT *et al.* 2020). Growth assays revealed that the SDL of *doa1Δ*, *slx5Δ*, *cdc4-1*, and *cdc7-4 GALCSE4* strains is suppressed when either *HHF1* or *HHF2* is deleted (Figures 3A and 3B and Table 2), while the SDL of *hir2Δ GALCSE4* is suppressed only when *HHF2* is deleted (Figure 3A and Table 2). These results suggest that the gene dosage of *H4* contributes to the SDL of mutants that exhibit defects in Cse4 proteolysis and mislocalize Cse4 to non-centromeric regions.

Reduced gene dosage of *H4* reduces the mislocalization of Cse4 in *psh1Δ* strains

The SDL phenotype and Cse4 proteolysis defect of *psh1Δ* strains are correlated with the mislocalization of Cse4 to non-centromeric regions (HEWAWASAM *et al.* 2010; RANJITKAR *et al.* 2010). So, we examined if the suppression of SDL in the *psh1Δ hhf1Δ* or *psh1Δ hhf2Δ GALCSE4* strains is due to reduced mislocalization of Cse4. We performed ChIP-qPCR to assay the localization of Cse4 using chromatin from wild type, *psh1Δ*, *hhf1Δ*, *hhf2Δ*, *psh1Δ hhf1Δ*, and *psh1Δ hhf2Δ* strains transiently overexpressing *GAL1-6His-3HA-CSE4*. In agreement with previously published data (HILDEBRAND AND BIGGINS 2016; HEWAWASAM *et al.* 2018; OHKUNI *et al.* 2020), we found that Cse4 enrichment at non-centromeric regions such as *RDS1*, *SLP1*,

297 *GUP2*, and *COQ3* is higher in the *psh1Δ* strain compared to the wild type strain (Figures 4A and
298 4B and S4A and S4B). In contrast, deletion of *HHF2* (*hhf2Δ*) in a wild type strain or when
299 combined with *psh1Δ* showed reduced levels of Cse4 enrichment at these regions (Figures 4A
300 and 4B). Results for ChIP-qPCR with the *hhf1Δ* strain also showed reduced levels of Cse4 at
301 non-centromeric loci similar to that observed for the *hhf2Δ* strain (Figure S4A and S4B).
302 Consistent with previous studies (HILDEBRAND AND BIGGINS 2016), we observed higher levels of
303 Cse4 at peri-centromeric regions in a *psh1Δ* strain (Figures 4C and S4C). However, we observed
304 reduced levels of Cse4 at peri-centromeric regions in *psh1Δ hhf1Δ* and *psh1Δ hhf2Δ* strains when
305 compared to the *psh1Δ* strain (Figures 4C and S4C). Localization of Cse4 to the centromere was
306 not significantly altered in *hhf1Δ*, *hhf2Δ*, *psh1Δ hhf1Δ*, and *psh1Δ hhf2Δ* strains (Figures 4C and
307 S4C). Based on these results, we conclude that reduced gene dosage of *H4* contributes to reduced
308 levels of Cse4 at non-centromeric and peri-centromeric regions in *psh1Δ* strains.

309 Scm3 is the primary chaperone for centromeric deposition of Cse4 and strains depleted
310 for Scm3 are not viable (CAMAHORT *et al.* 2007). However, overexpression of Cse4 can rescue
311 the growth of Scm3-depleted cells, suggesting that non-Scm3-based mechanisms can promote
312 centromeric deposition of Cse4 (HEWAWASAM *et al.* 2018). Our studies so far have shown that
313 reduced gene dosage of *H4* contributes to suppression of Cse4 mislocalization to non-
314 centromeric regions. We next asked if the reduced gene dosage of *H4* would affect the Scm3-
315 independent centromeric deposition of Cse4 by assaying the growth of Scm3-depleted cells that
316 overexpress Cse4. In these strains, expression of Scm3 is regulated by a galactose-inducible
317 promoter and is only expressed when grown in galactose medium, but not in glucose medium.
318 However, overexpression of Cse4 from a copper-inducible promoter can suppress the growth
319 defect caused by depletion of Scm3 on copper-containing medium (HEWAWASAM *et al.* 2018).

We constructed strains with deletion of *HHF2* and performed Western blot analysis to confirm the induced overexpression of Cse4 in these strains when grown in copper-containing medium (Figure 4D). Growth assays showed that deletion of *HHF2* resulted in poor growth of cells when Cse4 is overexpressed in Scm3-depleted strains (Figure 4E, glucose + 0.5mM Cu). We conclude that physiological levels of histone H4 are required for deposition of Cse4 at the centromere in cells depleted of Scm3 and for mislocalization of Cse4 to peri-centromeric and non-centromeric regions in *psh1Δ* strains.

Deletion of *HHF2* contributes to reduced stability of Cse4 in a *psh1Δ* strain

The SDL phenotype of a *psh1Δ GALCSE4* strain is associated with Cse4 mislocalization and higher stability of Cse4 (HEWAWASAM *et al.* 2010; RANJITKAR *et al.* 2010). The suppression of the *psh1Δ GALCSE4* SDL and the reduced mislocalization of Cse4 by *hhf2Δ* prompted us to examine the effect of *hhf2Δ* on Cse4 stability in wild type and *psh1Δ* strains. Protein stability assays showed that, in agreement with previous studies (HEWAWASAM *et al.* 2010; RANJITKAR *et al.* 2010), transiently expressed *GAL1-6His-3HA-CSE4* is highly stable in the *psh1Δ* strain when compared to that observed in a wild type strain. Stability of Cse4 was not significantly affected in the *hhf2Δ* strain when compared to the wild type strain. We observed reduced stability of Cse4 in the *psh1Δ hhf2Δ* strain compared to the *psh1Δ* strain (Figure 5A). These results show a correlation between suppression of SDL of *psh1Δ GALCSE4*, reduced mislocalization of Cse4 at non-centromeric regions, and reduced stability of Cse4 due to reduced gene dosage of *H4*.

Since defects in the ubiquitin-proteasome mediated proteolysis of Cse4 contribute to its increased stability (HEWAWASAM *et al.* 2010; RANJITKAR *et al.* 2010), we investigated if deletion of *HHF2* affects ubiquitination of Cse4 (Ub_n-Cse4) in a *psh1Δ* strain. Ubiquitin pull-down assays were done to determine the levels of Ub_n-Cse4 in wild type, *psh1Δ*, *hhf2*, and *psh1Δ hhf2Δ*

strains transiently overexpressing *GAL1-6His-3HA-CSE4*. Wild type strains expressing a non-tagged Cse4 or a mutant form of Cse4 ($cse4^{16KR}$) that cannot be ubiquitinated, where the 16 lysine residues are mutated to arginine, were used as negative controls. As previously reported (HEWAWASAM *et al.* 2010; RANJITKAR *et al.* 2010), levels of Ub_n-Cse4 were greatly reduced in the *psh1Δ* strain (38.2%±12.7) when compared to the wild type strain. The levels of Ub_n-Cse4 in the *psh1Δ hhf2Δ* strain (31.7%±12.3) were similar to the *psh1Δ* strain (Figure 5B). Interestingly, we found that levels of Ub_n-Cse4 were decreased in the *hhf2Δ* strain (65.3%±23.9) compared to the levels in the wild type strain (Figure 5B). We propose that reduced mislocalization of Cse4 and ubiquitin-independent proteolysis of Cse4 contribute to reduced stability of Cse4 in a *psh1Δ hhf2Δ GALCSE4* strain.

Defects in the Cse4-H4 interaction suppress the *psh1Δ GALCSE4* SDL

Our results so far have shown that reduced gene dosage of *H4* contributes to the reduced levels of Cse4 at non-centromeric and peri-centromeric regions and suppresses the SDL phenotype of *psh1Δ GALCSE4* strains. We hypothesized that defects in the interaction of H4 with Cse4 will also result in the suppression of the SDL phenotype of a *psh1Δ GALCSE4* strain. We used *hhf1* mutants with mutations either in the N-terminal lysines (*hhf1-10*) or in the histone fold domain (*hhf1-20*) that have been well characterized by genetic and biochemical analysis by the laboratory of Mitch Smith (SMITH *et al.* 1996; GLOWCZEWSKI *et al.* 2000). Defects in the formation of the Cse4-H4 dimer in the *hhf1-20* strain, but not the *hhf1-10* strain, are proposed to contribute to the suppression of the temperature sensitivity of *hhf1-20* but not *hhf1-10* strains by overexpression of Cse4. We deleted *PSH1* in the same genetic background as the *hhf1-10* and *hhf1-20* strains and transformed these strains with *GAL1-6His-3HA-CSE4* on a plasmid. Growth assays were performed in strains expressing *GAL1-6His-3HA-CSE4* in the presence of only one

366 histone *H3/H4* gene copy as either *HHT1/HHF1* (wild type), *HHT1/hhf1-10*, or *HHT1/hhf1-20*.
367 Compared to wild type strains with a single copy of genes encoding histones H3/H4,
368 *HHT1/HHF1 psh1Δ* strains display SDL when Cse4 is overexpressed, albeit at a less prominent
369 defect than that in the *psh1*Δ strain with two copies of the genes encoding H3/H4 (compare
370 Figure 6 to Figure 2A, *psh1Δ GALCSE4*). The relative decrease in SDL may be due to the
371 expression of a single copy of the genes encoding histones H3/H4 in the strain background. Our
372 results show that the *hhf1-20* mutant suppresses the SDL of *psh1Δ GALCSE4* strains while the
373 *hhf1-10* mutant does not (Figure 6). These findings suggest that the defect in the interaction of
374 mutant H4 with Cse4 contributes to the suppression of the *psh1Δ GALCSE4* SDL in the *hhf1-20*
375 strain.
376

DISCUSSION

Mislocalization of CENP-A and its homologs contributes to CIN in yeast, fly, and human cells (HEUN *et al.* 2006; AU *et al.* 2008; MISHRA *et al.* 2011; LACOSTE *et al.* 2014; ATHWAL *et al.* 2015; SHRESTHA *et al.* 2017) and overexpression and mislocalization of CENP-A is observed in many cancers (TOMONAGA *et al.* 2003; AMATO *et al.* 2009; LI *et al.* 2011; MCGOVERN *et al.* 2012; SUN *et al.* 2016; ZHANG *et al.* 2016). In this study, we performed the first genome-wide screen to identify deletion or temperature sensitive (*ts*) mutants that facilitate the mislocalization of Cse4 to non-centromeric regions. Deletion of either allele that encodes histone H4, *HHF1* and *HHF2*, were among the most prominent suppressors of *psh1Δ GALCSE4* SDL and we defined a role for gene dosage of histone H4 encoding genes in mislocalization of Cse4. The suppression of SDL is specific to deletion of genes encoding H4 as deletion of either copy of genes encoding histones H2A or H3 does not suppress the *psh1Δ GALCSE4* SDL. Deletion of *HHF1* or *HHF2* also suppresses the *GALCSE4* SDL of *slx5Δ*, *doa1Δ*, *hir2Δ*, *cdc4-1*, and *cdc7-4* strains. We hypothesize that reduced gene dosage of *H4* contributes to reduced mislocalization of Cse4 at peri-centromeric and non-centromeric regions, which in turn results in faster degradation of Cse4 not incorporated into chromatin and suppression of *psh1Δ GALCSE4* SDL. Based on the known defect in Cse4-H4 interaction in the *hhf1-20* strain and the suppression of *psh1Δ GALCSE4* SDL by *hhf1-20*, we propose that defects in the interaction of Cse4 with H4 reduce the association of Cse4 with chromatin. In summary, our genome-wide screen identified genes that contribute to Cse4 mislocalization and provided mechanistic insights into how reduced gene dosage of *H4* prevents mislocalization of Cse4 into non-centromeric regions.

The suppressor screen was performed under a condition with high levels of Cse4 overexpression induced from a *GAL1-6His-3HA-CSE4* plasmid, which contributes to mild

growth sensitivity even in wild type cells and this is further enhanced in *psh1Δ* strains (Figure 2). To reduce the number of false positives suppressors, we performed the screen with a *psh1Δ GAL1-6His-3HA-CSE4* strain grown on 2% galactose medium to achieve maximum levels of Cse4 overexpression. These growth conditions limited us from identifying partial suppressors such as deletion of *NHP10*, which encodes a subunit of the INO80 chromatin remodeling complex and was previously shown to suppress the *psh1Δ GALCSE4* SDL on medium with a lower concentration of galactose (0.1%) (HILDEBRAND AND BIGGINS 2016). While our screen did not identify *nhp10Δ*, it did identify two deletions and one mutant allele for genes which encode INO80 subunits and are evolutionarily conserved between yeast and human cells, Act1, Ies2, and Arp8 (POCH AND WINSOR 1997; SHEN *et al.* 2000; SHEN *et al.* 2003; TOSI *et al.* 2013). Secondary growth validation showed that *arp8Δ*, but not *act1-132* or *ies2Δ*, suppresses the *psh1Δ GALCSE4* SDL. The polyploid nature of the *arp8Δ* strain used in the screen precluded further study with this suppressor. The stringent growth conditions of the screen also prevented the identification of deletion of Cac2, a subunit of the CAF-1 complex, which promotes Cse4 incorporation at non-centromeric regions (HEWAWASAM *et al.* 2018). We determined that *cac2Δ* cannot suppress the *psh1Δ GAL1-6HIS-3HA-CSE4* SDL under the conditions used in our screen (data not shown).

The identification of both *hhf1Δ* and *hhf2Δ* as suppressors of *psh1Δ GALCSE4* SDL led us to examine how reduced gene dosage of *H4* contributes to the association of Cse4 with chromatin. A role for histone H4 in centromeric localization of Cse4 has been reported previously (DEYTER *et al.* 2017) however, a role for reduced gene dosage of *H4* in non-centromeric chromosome localization of Cse4 has not yet been reported. Previous studies have shown that mislocalization of Cse4 to non-centromeric regions contributes to the *GALCSE4* SDL in *psh1Δ*, *slx5Δ*, *doa1Δ*, *hir2Δ*, *cdc4-1*, and *cdc7-4* strains (HEWAWASAM *et al.* 2010; RANJITKAR

et al. 2010; AU *et al.* 2013; OHKUNI *et al.* 2016; CIFTCI-YILMAZ *et al.* 2018; AU *et al.* 2020; EISENSTATT *et al.* 2020). We determined that suppression of the *GALCSE4* SDL phenotype by *hhf1*Δ and *hhf2*Δ is not restricted to *psh1*Δ strains and is also observed in *slx5Δ*, *doa1Δ*, *hir2Δ*, *cdc4-1*, and *cdc7-4* strains. Genome-wide studies have shown that overexpressed Cse4 is significantly enriched at promoters and peri-centromeric regions in a *psh1*Δ strain (HILDEBRAND AND BIGGINS 2016). Our ChIP-qPCR data showed reduced levels of Cse4 at peri-centromeric and non-centromeric regions in *psh1Δ hhf1Δ* and *psh1Δ hhf2Δ* strains when compared to the *psh1Δ* strain.

The mislocalization of overexpressed Cse4 to non-centromeric regions contributes to highly stable Cse4 in *psh1Δ*, *slx5Δ*, *doa1Δ*, *hir2Δ*, *cdc4-1*, and *cdc7-4* strains (HEWAWASAM *et al.* 2010; RANJITKAR *et al.* 2010; AU *et al.* 2013; OHKUNI *et al.* 2016; CIFTCI-YILMAZ *et al.* 2018; AU *et al.* 2020; EISENSTATT *et al.* 2020). We reasoned that reduced mislocalization of Cse4 to non-centromeric regions in *psh1Δ hhf2*Δ strains may contribute to faster degradation of Cse4 in these strains. Our results showed that the proteolysis of Cse4 was indeed faster in *psh1*Δ *hhf2*Δ strains when compared to *psh1*Δ strain. Intriguingly, this was not due to increased ubiquitination of Cse4 (Ub_n-Cse4) in *psh1*Δ *hhf2*Δ strains. These results suggest a ubiquitin-independent mechanism for proteolysis of Cse4 in *hhf2Δ psh1Δ* strains. Ubiquitin-independent proteolysis has also been reported previously as $cse4^{16KR}$, in which all lysine residues are mutated to arginine, is not completely stabilized (COLLINS *et al.* 2004).

The suppression of SDL is specific to deletion of genes encoding histone H4 as deletion of genes encoding H2A or H3 do not suppress the *psh1Δ GALCSE4* SDL. These results suggest that interaction of H4 with Cse4 is the determining factor for association of Cse4 with chromatin. To test this hypothesis, we used the *hhf1-20* mutant strain in which the formation of the Cse4-H4

dimer is impaired and the *hhf1-10* mutant, which does not show this defect (SMITH *et al.* 1996; GLOWCZEWSKI *et al.* 2000). The *hhf1* mutant strains lack the *HHT2/HHF2* allele and express only a single copy of *H3/H4*, which is either wild type (*HHT1/HHF1*), *hhf1-10* (*HHT1/hhf1-10*), or *hhf1-20* (*HHT1/hhf1-20*). In this strain background, the *psh1Δ GALCSE4* SDL was less severe compared to results in our strains with wild type copies of both *HHT1/HHF1* and *HHT2/HHF2* (Figure 2). Despite this, we were able to distinguish a suppression of the growth defect in the *hhf1-20 psh1Δ GALCSE4* strain and conclude that *hhf1-20*, but not *hhf1-10*, suppresses the *psh1Δ GALCSE4* SDL. Interestingly, the *hhf1-10 psh1Δ GALCSE4* strain displayed more lethality. The N-terminal lysine residues on histone H4 are acetylated and the *hhf1-10* mutations mimic the acetylated state of the lysine residues (K to Q). We propose that hyperacetylation of histone H4 may promote higher mislocalization of Cse4 and a more severe *hhf1-10 psh1Δ GALCSE4* SDL. A recent study showed that mutation of histone H4 (H4R36A) contributes to defects in ubiquitin-mediated proteolysis and mislocalization of Cse4 to non-centromeric regions (DEYTER *et al.* 2017). Based on our results, we predict that while the H4R36A mutant contributes to the Cse4-Psh1 interaction, it will not be defective for interaction with Cse4. Taken together, our results show that defects in the interaction of H4 with Cse4 contributes to suppression of the SDL in *hhf1-20 psh1Δ GALCSE4* strain. It will be of interest to perform reciprocal studies with *cse4* mutants with or without defects in the interaction with H4 to confirm that Cse4-H4 facilitates the incorporation of Cse4 into chromatin.

In summary, our genome-wide screen has identified suppressors of *psh1Δ GALCSE4* SDL with deletions of either allele that encodes histone H4 (*HHF1* and *HHF2)* as among the most prominent suppressors. We present several experimental evidences to support our conclusion that reduced gene dosage of *H4* contributes to reduced mislocalization of Cse4 at

peri-centromeric and non-centromeric regions, which in turn results in faster degradation of Cse4 and suppression of the *psh1Δ GALCSE4* SDL. The suppression of SDL by *hhf1*Δ and *hhf2*Δ is not limited to *psh1*Δ *GALCSE4* but is also observed in other mutants that exhibit *GALCSE4* SDL. Most importantly, our results with the *hhf1-20* mutant, which is defective in interaction with Cse4, showed that the Cse4-H4 interaction is essential not only for centromeric association of Cse4, but also for non-centromeric localization of Cse4. Future studies will allow us to understand how defects in the interaction of Cse4 with H4 contribute to suppression of Cse4 mislocalization and the role of other suppressors identified in the screen. These studies are important from a clinical standpoint given the poor prognosis of CENP-A overexpressing cancers (TOMONAGA *et al.* 2003; AMATO *et al.* 2009; LI *et al.* 2011; MCGOVERN *et al.* 2012; SUN *et al.* 2016; ZHANG *et al.* 2016).

ACKNOWLEDGEMENTS

We gratefully acknowledge Jennifer Gerton and Mitch Smith for reagents, Kathy McKinnon of the National Cancer Institute Vaccine Branch FACS Core for assistance with FACS analysis, Anthony Dawson for strain construction, and the members of the Basrai laboratory for helpful discussions and comments on the manuscript. MAB is supported by the NIH Intramural Research Program at the National Cancer Institute. This research was also supported by grants from the National Institutes of Health to CB and MC (R01HG005853) and from the Canadian Institute of Health Research to CB (FDN-143264). CB is a fellow in the Canadian Institute for Advanced Research (CIFAR, https://www.cifar.ca/) Fungal Kingdom: Threats and Opportunities. The funders had no role in study design, data collection and analysis, decision to publish, or preparation of the manuscript.

FIGURE LEGENDS

Figure 1. A genome-wide screen identified suppressors of the *psh1Δ GALCSE4* SDL. A. Schematic for the genome-wide screen. A *psh1Δ* strain (YMB10478) transformed with *GAL1-6His-3HA-CSE4* (pMB1458) was mated to an array of non-essential gene deletions and an array of conditional alleles of essential genes. Growth of the haploid meiotic progeny plated in quadruplicate was visually scored on glucose-and galactose-containing media grown at 30°C for non-essential and 26°C for essential gene mutant strains. Ninety-two genes were identified as growing better on galactose-containing media than the *psh1Δ GALCSE4* strain. Thirty-eight candidate genes were selected for confirmation of suppression of lethality. **B. Representative plates from the genome-wide screen.** Shown is Plate 01 of the non-essential gene deletion array. The mutant strains were spotted in quadruplicate on selective media plates containing glucose (top) or galactose (bottom). Red boxes (top box is *hap3Δ*; bottom box is *hhf1Δ*) highlight mutant strains that displayed improved growth on galactose-containing plates compared to the *psh1Δ GALCSE4* control strain (perimeter of plate) and did not show a growth defect or improved growth on the glucose plates.

Figure 2. Deletion of *H4* genes suppresses the *psh1Δ GALCSE4* SDL. Three independent isolates for each strain were assayed and shown is a representative for each. **A. The *psh1Δ GALCSE4* SDL is suppressed by deletion of *HHF1* or *HHF2*.** Growth assays of wild type, *psh1Δ*, *hhf1Δ*, *hhf2Δ*, *psh1Δ hhf1Δ*, and *psh1Δ hhf2Δ* strains with empty vector (pMB433; YMB9802, YMB10478, YMB10825, YMB11166, YMB10821, and YMB10823 respectively) or *GAL1-6His-3HA-CSE4* (pMB1458; YMB9803, YMB10479, YMB10937, YMB10938, YMB10822, and YMB10824 respectively). Cells were spotted in five-fold serial dilutions on glucose (2% final concentration) or raffinose/galactose (2% final concentration each) media

selective for the plasmid and grown at 30°C for three to five days. **B. The *psh1Δ GALCSE4* SDL suppression is linked to the *hhf1Δ* and *hhf2Δ* alleles.** Growth assays of *psh1Δ hhf1Δ* (YMB10822) and *psh1Δ hhf2Δ* (YMB10824) strains with *GAL1-6His-3HA-CSE4* (pMB1458) transformed with empty vector (pRS425) or a plasmid containing wild type *HHF1* (pMB1928) or *HHF2* (pMB1929). Strains were assayed as described above in (A). **C.** and **D. Deletion of genes encoding histones H2A (C) or H3 (D) does not suppress the SDL of a *psh1Δ GALCSE4* strain.** Growth assays of wild type, *psh1Δ*, (E) *hta1Δ*, *hta2Δ*, *psh1Δ hta1Δ*, *psh1Δ hta2Δ*, (F) *hht1Δ*, *hht2Δ*, *psh1Δ hht1Δ*, and *psh1Δ hht1Δ* strains with empty vector (pMB433; YMB9802, YMB10478, YMB11258, YMB11266, YMB11260, YMB11268, YMB11274, YMB11282, YMB11276, and YMB11284 respectively) or *GAL1-6His-3HA-CSE4* (pMB1458: YMB9803, YMB10479, YMB11262, YMB11270, YMB11264, YMB11272, YMB11278, YMB11286, YMB11280, and YMB11288 respectively). Strains were assayed as described above in (A).

Figure 3. Deletion of *HHF1* or *HHF2* suppresses the SDL of mutant strains that exhibit *GALCSE4*-induced SDL and Cse4 mislocalization. Three independent isolates of each strain were assayed and shown is a representative for each. **A. Reduced gene dosage of *H4* suppresses the SDL of *slx5Δ*, *doa1Δ*, and *hir2Δ GALCSE4* strains.** Growth assays of wild type (YMB9804), *hhf1Δ* (YMB10937), *hhf2Δ* (YMB10938), *slx5Δ* (YMB10963), *slx5Δ hhf1Δ* (YMB11046), *slx5Δ hhf2Δ* (YMB11047), *doa1Δ* (YMB11032), *doa1Δ hhf1Δ* (YMB11050), *doa1Δ hhf2Δ* (YMB11053), *hir2Δ* (YMB8332), *hir2Δ hhf1Δ* (YMB11105), *hir2Δ hhf2Δ* (YMB11107) strains expressing *GAL1-6HIS-3HA-CSE4* (pMB1458). Cells were spotted in five-fold serial dilutions on glucose (2% final concentration) or raffinose/galactose (2% final

concentration each) media selective for the plasmid and grown at 30°C for three to five days. **B. Deletion of *HHF1* or *HHF2* suppresses the SDL of *cdc4-1* and *cdc7-4 GALCSE4* strains.** Growth assays of wild type (YMB9804), *hhf1Δ* (YMB10937), *hhf2Δ* (YMB10938), *cdc4-1* (YMB9756), *cdc4-1 hhf1Δ* (YMB11051), *cdc4-1 hhf2Δ* (YMB11054), *cdc7-4* (YMB9760), *cdc7-4 hhf1Δ* (YMB11052), and *cdc7-4 hhf2Δ* (YMB11055) with *GAL1-6His-3HA-CSE4* (pMB1458). Strains were assayed as described above in (A) and grown at 23°C.

Figure 4. Deletion of *HHF2* reduces enrichment of Cse4 at peri-centromeric and non-centromeric regions. (A-C) ChIP-qPCR was performed on chromatin lysate from wild type (YMB9804), *psh1Δ* (YMB10479), *hhf2Δ* (YMB10938), and *psh1Δ hhf2Δ* (YMB10824) strains transiently expressing *GAL1-6His-3HA-CSE4* (pMB1458). Enrichment of 6His-3HA-Cse4 is shown as a fold over wild type. Displayed are the mean of two independent experiments. Error bars represent standard deviation of the mean. ***p*-value<0.0099, **p*-value<0.09, ns=not significant. **A.** and **B. Levels of Cse4 enrichment at non-centromeric regions are reduced in a *hhf2Δ* strain.** Enrichment of 6His-3HA-Cse4 at (A) *RDS1*, *SLP1*, *COQ3*, *GUP2*, and (B) *ACT1*, *SAP1*, *PHO5*, *FIG4*, and *UGA3*. **C. Levels of Cse4 at peri-centromeric regions, but not at the core centromere, are significantly reduced when *HHF2* is deleted.** Top: A diagram of the peri-centromere and centromere of Chromosome III analyzed by ChIP-qPCR. Horizontal lines represent the regions amplified. Bottom: Enrichment of 6His-3HA-Cse4 at the core centromere and at the left and right peri-centromeric regions on Chromosome III. **D. Cse4 is expressed from a copper-inducible promoter in *hhf2Δ* strains depleted of Scm3.** Strains from (D) were grown to logarithmic phase in liquid media selective for the plasmid. Cells were induced with 0.5 mM copper for 2 hours and protein lysates were collected and analyzed by

563 Western blot against Cse4 and Tub2 as a loading control. E: empty vector; C: copper inducible
564 Cse4; -: no copper; +: 0.5 mM copper. **E. Deletion of *HHF2* reduces Cse4 deposition at the**
565 **centromere in cells depleted of Scm3.** Growth assays of strains in which Scm3 is expressed
566 from a galactose inducible promoter and Cse4 expressed from a copper-inducible promoter. Wild
567 type and *hhf2Δ* with empty vector (pSB17; JG1589 and YMB11252 respectively) or a plasmid
568 with copper inducible Cse4 (pSB873; JG1690 and YMB11254 respectively) were plated in five-
569 fold serial dilutions on media plates selective for the plasmid with raffinose/galactose (2% final
570 concentration each) or glucose (2 % final concentration) and with or without copper (0.5 mM
571 final concentration). Plates were grown for three to five days at 30°C. Two independent
572 transformants were tested and a representative image is shown.
573
574 **Figure 5. Deletion of *HHF2* contributes to reduced stability and ubiquitin-independent**
575 **proteolysis of Cse4 in a *psh1Δ* strain. A. *hhf2Δ* strains contribute to reduced stability of**
576 **Cse4 in a *psh1Δ* strain.** Western blot analysis of protein extracts from wild type (YMB9804),
577 *psh1Δ* (YMB10479), *hhf2Δ* (YMB10938), and *psh1Δ hhf2Δ* (YMB10824) strains transiently
578 expressing *GAL1-6His-3HA-CSE4* (pMB1458). Cells were grown to logarithmic phase in media
579 selective for the plasmid and containing raffinose (2% final concentration) and induced with
580 galactose (2% final concentration) for 4 hours. Cultures were treated with cycloheximide (CHX,
581 10 µg/mL) and analyzed at the indicated time points. Extracts were analyzed by Western blot
582 against HA (Cse4) and Tub2 as a loading control. Levels of 6His-3HA-Cse4 were normalized to
583 Tub2 and the quantification of the percent remaining 6His-3HA-Cse4 after CHX treatment is
584 shown in the graph. Error bars represent the SEM of two independent experiments. **B. Deletion**
585 **of *HHF2* does not increase ubiquitination of Cse4 in a *psh1Δ* strain.** Ubiquitin-pull down

assays were performed using protein extracts from wild type strains (BY4741) with no tag (pMB433) or expressing *cse4*^{16KR} (pMB1892) and from wild type (YMB9804), *psh1Δ* (YMB10479), *hhf2Δ* (YMB10938), and *psh1Δ hhf2Δ* (YMB10824) strains expressing *GAL1-6His-3HA-CSE4* (pMB1458). Lysates were incubated with Tandem Ubiquitin Binding Entity beads (LifeSensors) prior to analysis of ubiquitin-enriched samples by Western blot against HA and input samples against HA and Tub2 as a loading control. Poly-ubiquitinated Cse4 (Ub_n-Cse4) is indicated by the bracket. HA levels in input samples were normalized to Tub2 levels and quantification of levels of Ub_n-Cse4 were normalized to the levels of Cse4 in the input. The percentage of Ub_n-Cse4 from two independent experiments with standard error is shown.

Figure 6: Mutations in the histone fold domain of histone H4 suppress the SDL phenotype of a *psh1Δ GALCSE4* strain. Growth assays of wild type (MSY559), *psh1Δ* (YMB11346), *hhf1-10* (MSY535), *hhf1-20* (MSY534), *psh1Δ hhf1-10* (YMB11347), and *psh1Δ hhf1-20* (YMB11348) with empty vector (pMB433) or expressing *GAL1-6His-3HA-CSE4* (pMB1458). Cells were plated in five-fold serial dilutions on selective media plates containing either glucose (2% final concentration) or raffinose/galactose (2% final concentration each). Plates were incubated at 30°C for three to five days. Three independent transformants were tested and a representative image is shown.

TABLES

TABLE 1. Candidate double mutant strains with the indicated mutant allele combined with *psh1Δ GALCSE4* were generated and used for secondary validation using growth assays. Indicated is the allele analyzed, systematic name, gene name, standard name, visual scoring from the primary screen for growth score (from one to four) and colony score (from one to four), and suppression of SDL (Y: SDL was suppressed; N: SDL was not suppressed; Partial: SDL was partially suppressed).

Allele	Systematic Name	Gene Name	Standard Name	Growth Score	Colony Score	SDL Suppression
Non-essential						
hhf1Δ	YBR009C	*HHF1*	Histone H4	3	4	Y
hhf2Δ	YNL030W	*HHF2*	Histone H4	3	4	Y
ies2Δ	YNL215W	*IES2*	Ino Eighty Subunit	2	3	N
arp8Δ	YOR141C	*ARP8*	Actin-Related Protein	3	4	Y
swc5Δ	YBR231C	*SWC5*	SWr Complex	1	4	N
eaf1Δ	YDR359C	*EAF1*	Esa1p-Associated Factor	2	3	Partial
eap1Δ	YKL204W	*EAP1*	EIF4E-Associated Protein	2	4	Y
cse2Δ	YNR010W	*CSE2*	Chromosome SEgregation	2	3	Partial
cse2Δ_tsa	YNR010W	*CSE2*	Chromosome SEgregation	3	3	Y
mrm2Δ	YGL136C	*MRM2*	Mitochondrial rRNA Methyl transferase	2	3	N
hap3Δ	YBL021C	*HAP3*	Heme Activator Protein	3	4	Partial
hap5Δ	YOR358W	*HAP5*	Heme Activator Protein	3	4	Y
rpl6bΔ	YLR448W	*RPL6B*	Ribosomal Protein of the Large subunit	2	3	Y
rad4Δ	YER162C	*RAD4*	RADiation sensitive	2	3	Partial
rad14Δ	YMR201C	*RAD14*	RADiation sensitive	2	2	Y
Essential						
act1-132	YFL039C	*ACT1*	ACTin	3	4	N
mob1-5001	YIL106W	*MOB1*	Mps One Binder	4	4	Y
tbf1-5001	YPL128C	*TBF1*	TTAGGG repeat-Binding Factor	3	4	Y
csl4-5001	YNL232W	*CSL4*	Cep1 Synthetic Lethal	4	4	Y
pop4-5001	YBR257W	*POP4*	Processing Of Precursor RNAs	4	4	Y
orc1-5001	YML065W	*ORC1*	Origin Recognition Complex	4	4	Y
orc6-5001	YHR118C	*ORC6*	Origin Recognition Complex	4	4	Y
cft2-1	YLR115W	*CFT2*	Cleavage Factor Two	3	4	Partial
cft2-5001	YLR115W	*CFT2*	Cleavage Factor Two	4	4	Y
clp1-5001	YOR250C	*CLP1*	CLeavage/Polyadenylation factor Ia subunit	4	3	Y
ipa1-5001	YJR141W	*IPA1*	Important for cleavage and PolyAdenylation	3	4	Y
hrp1-1	YOL123W	*HRP1*	Heterogenous nuclear RibonucleoProtein	2	4	Y
rpb5-5001	YBR154C	*RPB5*	RNA Polymerase B	4	4	Y
rpc17-5001	YJL011C	*RPC17*	RNA Polymerase C	4	4	Y
pol31-5001	YJR006W	*POL31*	POLymerase	4	4	Y
srp54-5001	YPR088C	*SRP54*	Signal Recognition Particle 54-kD subunit	4	4	Y
dbp6-5001	YNR038W	*DBP6*	Dead Box Protein	4	4	Y

dbp9-5001	YLR276C	*DBP9*	Dead Box Protein	4	4	Y
yef3-f650s	YLR249W	*YEF3*	Yeast Elongation Factor	2	4	Y
cdc5-1	YMR001C	*CDC5*	Cell Division Cycle	2	4	Y
cdc31-1	YOR257W	*CDC31*	Cell Division Cycle	2	4	Y
hrr25-5001	YPL204W	*HRR25*	HO and Radiation Repair	3	4	Y
ost2-5001	YOR103C	*OST2*	OligoSaccharylTransferase	4	4	Y

TABLE 2. Summary of the SDL growth phenotypes of mutants that exhibit SDL with *GALCSE4* and combined with *hhf1Δ* or *hhf2Δ*. Shown is the protein function, relevant strain genotype, and growth with *GALCSE4*. Wild type growth is indicated as ++; SDL as --- and extent of suppression (++ or +++).

Protein Function	**Relevant Strain Genotype**	**Growth with *GALCSE4***
	WT	++
Histone H4	*hhf1Δ*	+++
	hhf2Δ	+++
Histone H2A	*hta1Δ*	++
	hta2Δ	++
Histone H3	*hht1Δ*	++
	hht2Δ	++
E3 Ubiquitin Ligase	*psh1Δ*	---
	psh1Δ hhf1Δ	+++
	psh1Δ hhf2Δ	+++
	psh1Δ hhf1Δ + HHF1	---
	psh1Δ hhf2Δ + HHF2	---
	psh1Δ hta1Δ	---
	psh1Δ hta2Δ	---
	psh1Δ hht1Δ	---
	psh1Δ hht2Δ	---
SUMO-Targeted Ubiquitin Ligase	*slx5Δ*	--
	slx5Δ hhf1Δ	+++
	slx5Δ hhf2Δ	+++
Ubiquitin Binding	*doa1Δ*	---
	doa1Δ hhf1Δ	+++
	doa1Δ hhf2Δ	+++

HIR Nucleosome Binding Complex	*hir2Δ*	--
	hir2Δ hhf1Δ	-
	hir2Δ hhf2Δ	++
F-box of the SCF Complex	*cdc4-1*	--
	cdc4-1 hhf1Δ	+++
	cdc4-1 hhf2Δ	+++
Dbf4-Dependent Kinase	*cdc7-4*	---
	cdc7-4 hhf1Δ	++
	cdc7-4 hhf2Δ	++

617

618

CITATIONS

Allshire, R. C., and G. H. Karpen, 2008 Epigenetic regulation of centromeric chromatin: old dogs, new tricks? Nat Rev Genet 9**:** 923-937.

Amato, A., T. Schillaci, L. Lentini and A. Di Leonardo, 2009 CENPA overexpression promotes genome instability in pRb-depleted human cells. Mol Cancer 8**:** 119.

Athwal, R. K., M. P. Walkiewicz, S. Baek, S. Fu, M. Bui *et al.*, 2015 CENP-A nucleosomes localize to transcription factor hotspots and subtelomeric sites in human cancer cells. Epigenetics Chromatin 8**:** 2.

Au, W. C., M. J. Crisp, S. Z. DeLuca, O. J. Rando and M. A. Basrai, 2008 Altered dosage and mislocalization of histone H3 and Cse4p lead to chromosome loss in Saccharomyces cerevisiae. Genetics 179**:** 263-275.

Au, W. C., A. R. Dawson, D. W. Rawson, S. B. Taylor, R. E. Baker *et al.*, 2013 A Novel Role of the N-Terminus of Budding Yeast Histone H3 Variant Cse4 in Ubiquitin-Mediated Proteolysis. Genetics 194**:** 513-518.

Au, W. C., T. Zhang, P. K. Mishra, J. R. Eisenstatt, R. L. Walker *et al.*, 2020 Skp, Cullin, F-box (SCF)-Met30 and SCF-Cdc4-Mediated Proteolysis of CENP-A Prevents Mislocalization of CENP-A for Chromosomal Stability in Budding Yeast. PLoS Genet 16**:** e1008597.

Biggins, S., 2013 The Composition, Functions, and Regulation of the Budding Yeast Kinetochore. Genetics 194**:** 817-846.

Boltengagen, M., A. Huang, A. Boltengagen, L. Trixl, H. Lindner *et al.*, 2016 A novel role for the histone acetyltransferase Hat1 in the CENP-A/CID assembly pathway in Drosophila melanogaster. Nucleic Acids Res 44**:** 2145-2159.

641 Burrack, L. S., and J. Berman, 2012 Flexibility of centromere and kinetochore structures. Trends
642 Genet 28**:** 204-212.
643 Camahort, R., B. Li, L. Florens, S. K. Swanson, M. P. Washburn *et al.*, 2007 Scm3 is essential to
644 recruit the histone H3 variant Cse4 to centromeres and to maintain a functional
645 kinetochore. Mol Cell 26**:** 853-865.
646 Chen, C. C., M. L. Dechassa, E. Bettini, M. B. Ledoux, C. Belisario *et al.*, 2014 CAL1 is the
647 Drosophila CENP-A assembly factor. J Cell Biol 204**:** 313-329.
648 Cheng, H., X. Bao, X. Gan, S. Luo and H. Rao, 2017 Multiple E3s promote the degradation of
649 histone H3 variant Cse4. Sci Rep 7**:** 8565.
650 Cheng, H., X. Bao and H. Rao, 2016 The F-box Protein Rcy1 Is Involved in the Degradation of
651 Histone H3 Variant Cse4 and Genome Maintenance. J Biol Chem 291**:** 10372-10377.
652 Chereji, R. V., J. Ocampo and D. J. Clark, 2017 MNase-Sensitive Complexes in Yeast:
653 Nucleosomes and Non-histone Barriers. Mol Cell 65**:** 565-577 e563.
654 Choy, J. S., P. K. Mishra, W. C. Au and M. A. Basrai, 2012 Insights into assembly and
655 regulation of centromeric chromatin in Saccharomyces cerevisiae. Biochim Biophys Acta
656 1819**:** 776-783.
657 Ciftci-Yilmaz, S., W. C. Au, P. K. Mishra, J. R. Eisenstatt, J. Chang *et al.*, 2018 A Genome-
658 Wide Screen Reveals a Role for the HIR Histone Chaperone Complex in Preventing
659 Mislocalization of Budding Yeast CENP-A. Genetics 210**:** 203-218.
660 Cole, H. A., J. Ocampo, J. R. Iben, R. V. Chereji and D. J. Clark, 2014 Heavy transcription of
661 yeast genes correlates with differential loss of histone H2B relative to H4 and queued
662 RNA polymerases. Nucleic Acids Res 42**:** 12512-12522.

663 Collins, K. A., S. Furuyama and S. Biggins, 2004 Proteolysis contributes to the exclusive
664 centromere localization of the yeast Cse4/CENP-A histone H3 variant. Curr Biol 14**:**
665 1968-1972.
666 Costanzo, M., B. VanderSluis, E. N. Koch, A. Baryshnikova, C. Pons *et al.*, 2016 A global
667 genetic interaction network maps a wiring diagram of cellular function. Science 353.
668 Deyter, G. M., and S. Biggins, 2014 The FACT complex interacts with the E3 ubiquitin ligase
669 Psh1 to prevent ectopic localization of CENP-A. Genes Dev 28**:** 1815-1826.
670 Deyter, G. M., E. M. Hildebrand, A. D. Barber and S. Biggins, 2017 Histone H4 Facilitates the
671 Proteolysis of the Budding Yeast CENP-ACse4 Centromeric Histone Variant. Genetics
672 205**:** 113-124.
673 Eisenstatt, J. R., L. Boeckmann, W. C. Au, V. Garcia, L. Bursch *et al.*, 2020 Dbf4-Dependent
674 Kinase (DDK)-Mediated Proteolysis of CENP-A Prevents Mislocalization of CENP-A in
675 Saccharomyces cerevisiae. G3 (Bethesda).
676 Foltz, D. R., L. E. Jansen, A. O. Bailey, J. R. Yates, 3rd, E. A. Bassett *et al.*, 2009 Centromere-
677 specific assembly of CENP-a nucleosomes is mediated by HJURP. Cell 137**:** 472-484.
678 Fujita, Y., T. Hayashi, T. Kiyomitsu, Y. Toyoda, A. Kokubu *et al.*, 2007 Priming of centromere
679 for CENP-A recruitment by human hMis18alpha, hMis18beta, and M18BP1. Dev Cell
680 12**:** 17-30.
681 Glowczewski, L., P. Yang, T. Kalashnikova, M. S. Santisteban and M. M. Smith, 2000 Histone-
682 histone interactions and centromere function. Mol Cell Biol 20**:** 5700-5711.
683 Heun, P., S. Erhardt, M. D. Blower, S. Weiss, A. D. Skora *et al.*, 2006 Mislocalization of the
684 Drosophila centromere-specific histone CID promotes formation of functional ectopic
685 kinetochores. Dev Cell 10**:** 303-315.

686 Hewawasam, G., M. Shivaraju, M. Mattingly, S. Venkatesh, S. Martin-Brown *et al.*, 2010 Psh1
687 is an E3 ubiquitin ligase that targets the centromeric histone variant Cse4. Mol Cell 40**:**
688 444-454.
689 Hewawasam, G. S., K. Dhatchinamoorthy, M. Mattingly, C. Seidel and J. L. Gerton, 2018
690 Chromatin assembly factor-1 (CAF-1) chaperone regulates Cse4 deposition into
691 chromatin in budding yeast. Nucleic Acids Res 46**:** 4440-4455.
692 Hewawasam, G. S., M. Mattingly, S. Venkatesh, Y. Zhang, L. Florens *et al.*, 2014
693 Phosphorylation by casein kinase 2 facilitates Psh1 protein-assisted degradation of Cse4
694 protein. J Biol Chem 289**:** 29297-29309.
695 Hildebrand, E. M., and S. Biggins, 2016 Regulation of Budding Yeast CENP-A levels Prevents
696 Misincorporation at Promoter Nucleosomes and Transcriptional Defects. PLoS Genet 12**:**
697 e1005930.
698 Kastenmayer, J. P., L. Ni, A. Chu, L. E. Kitchen, W. C. Au *et al.*, 2006 Functional genomics of
699 genes with small open reading frames (sORFs) in S. cerevisiae. Genome Res 16**:** 365-
700 373.
701 Kitagawa, K., and P. Hieter, 2001 Evolutionary concervation between budding yeast and human
702 kinetochores. Nature Reviews Molecular Cellular Biology 2**:** 678-687.
703 Lacoste, N., A. Woolfe, H. Tachiwana, A. V. Garea, T. Barth *et al.*, 2014 Mislocalization of the
704 centromeric histone variant CenH3/CENP-A in human cells depends on the chaperone
705 DAXX. Mol Cell 53**:** 631-644.
706 Li, Y., Z. Zhu, S. Zhang, D. Yu, H. Yu *et al.*, 2011 ShRNA-targeted centromere protein A
707 inhibits hepatocellular carcinoma growth. PLoS One 6**:** e17794.

Maddox, P. S., K. D. Corbett and A. Desai, 2012 Structure, assembly and reading of centromeric chromatin. Curr Opin Genet Dev 22**:** 139-147.

McGovern, S. L., Y. Qi, L. Pusztai, W. F. Symmans and T. A. Buchholz, 2012 Centromere protein-A, an essential centromere protein, is a prognostic marker for relapse in estrogen receptor-positive breast cancer. Breast Cancer Res 14**:** R72.

McKinley, K. L., and I. M. Cheeseman, 2016 The molecular basis for centromere identity and function. Nat Rev Mol Cell Biol 17**:** 16-29.

Mishra, P. K., W. C. Au, J. S. Choy, P. H. Kuich, R. E. Baker *et al.*, 2011 Misregulation of Scm3p/HJURP causes chromosome instability in Saccharomyces cerevisiae and human cells. PLoS Genet 7**:** e1002303.

Mizuguchi, G., H. Xiao, J. Wisniewski, M. M. Smith and C. Wu, 2007 Nonhistone Scm3 and histones CenH3-H4 assemble the core of centromere-specific nucleosomes. Cell 129**:** 1153-1164.

Moreno-Moreno, O., M. Torras-Llort and F. Azorin, 2006 Proteolysis restricts localization of CID, the centromere-specific histone H3 variant of Drosophila, to centromeres. Nucleic Acids Res 34**:** 6247-6255.

Ohkuni, K., R. Abdulle and K. Kitagawa, 2014 Degradation of centromeric histone H3 variant Cse4 requires the Fpr3 peptidyl-prolyl Cis-Trans isomerase. Genetics 196**:** 1041-1045.

Ohkuni, K., E. Suva, W. C. Au, R. L. Walker, R. Levy-Myers *et al.*, 2020 Deposition of Centromeric Histone H3 Variant CENP-A/Cse4 into Chromatin Is Facilitated by Its C-Terminal Sumoylation. Genetics 214**:** 839-854.

729 Ohkuni, K., Y. Takahashi, A. Fulp, J. Lawrimore, W. C. Au *et al.*, 2016 SUMO-Targeted
730 Ubiquitin Ligase (STUbL) Slx5 regulates proteolysis of centromeric histone H3 variant
731 Cse4 and prevents its mislocalization to euchromatin. Mol Biol Cell.
732 Pidoux, A. L., E. S. Choi, J. K. Abbott, X. Liu, A. Kagansky *et al.*, 2009 Fission yeast Scm3: A
733 CENP-A receptor required for integrity of subkinetochore chromatin. Mol Cell 33**:** 299-
734 311.
735 Poch, O., and B. Winsor, 1997 Who's Who among the Saccharomyces cerevisiae Actin-Related
736 Proteins? A Classification and Nomenclature Proposal for a Large Family. Yeast 13**:**
737 1053-1058.
738 Ranjitkar, P., M. O. Press, X. Yi, R. Baker, M. J. MacCoss *et al.*, 2010 An E3 ubiquitin ligase
739 prevents ectopic localization of the centromeric histone H3 variant via the centromere
740 targeting domain. Mol Cell 40**:** 455-464.
741 Shen, X., G. Mizuguchi, A. Hamiche and C. Wu, 2000 A chromatin remodelling complex
742 involved in transcription and DNA processing. Nature 406**:** 541-544.
743 Shen, X., R. Ranallo, E. Choi and C. Wu, 2003 Inolvement of Actin-Related Proteins in ATP-
744 Dependent Chromatin Remodeling. Mol Cell 12**:** 147-155.
745 Shrestha, R. L., G. S. Ahn, M. I. Staples, K. M. Sathyan, T. S. Karpova *et al.*, 2017
746 Mislocalization of centromeric histone H3 variant CENP-A contributes to chromosomal
747 instability (CIN) in human cells. Oncotarget 8**:** 46781-46800.
748 Shuaib, M., K. Ouararhni, S. Dimitrov and A. Hamiche, 2010 HJURP binds CENP-A via a
749 highly conserved N-terminal domain and mediates its deposition at centromeres. Proc
750 Natl Acad Sci U S A 107**:** 1349-1354.

751 Smith, M. M., H. Yang, M. S. Santisteban, P. W. Boone, A. T. Goldstein *et al.*, 1996 A Novel
752 Histone H4 Mutant Defective in Nuclear Division
753 and Mitotic Chromosome Transmission. Mol Cell Biol 16**:** 1017-1026.
754 Stoler, S., K. Rogers, S. Weitze, L. Morey, M. Fitzgerald-Hayes *et al.*, 2007 Scm3, an essential
755 Saccharomyces cerevisiae centromere protein required for G2/M progression and Cse4
756 localization. Proc Natl Acad Sci U S A 104**:** 10571-10576.
757 Sun, X., P. L. Clermont, W. Jiao, C. D. Helgason, P. W. Gout *et al.*, 2016 Elevated expression of
758 the centromere protein-A(CENP-A)-encoding gene as a prognostic and predictive
759 biomarker in human cancers. Int J Cancer 139**:** 899-907.
760 Tomonaga, T., K. Matsushita, S. Yamaguchi, T. Oohashi, H. Shimada *et al.*, 2003
761 Overexpression and mistargeting of centromere protein-A in human primary colorectal
762 cancer. Cancer Res 63**:** 3511-3516.
763 Tosi, A., C. Haas, F. Herzog, A. Gilmozzi, O. Berninghausen *et al.*, 2013 Structure and Subunit
764 Topology of the INO80 Chromatin Remodeler and Its Nucleosome Complex. Cell 154**:**
765 1207-1219.
766 Verdaasdonk, J. S., and K. Bloom, 2011 Centromeres: unique chromatin structures that drive
767 chromosome segregation. Nat Rev Mol Cell Biol 12**:** 320-332.
768 Williams, J. S., T. Hayashi, M. Yanagida and P. Russell, 2009 Fission yeast Scm3 mediates
769 stable assembly of Cnp1/CENP-A into centromeric chromatin. Mol Cell 33**:** 287-298.
770 Zhang, W., J. H. Mao, W. Zhu, A. K. Jain, K. Liu *et al.*, 2016 Centromere and kinetochore gene
771 misexpression predicts cancer patient survival and response to radiotherapy and
772 chemotherapy. Nat Commun 7**:** 12619.
773

A

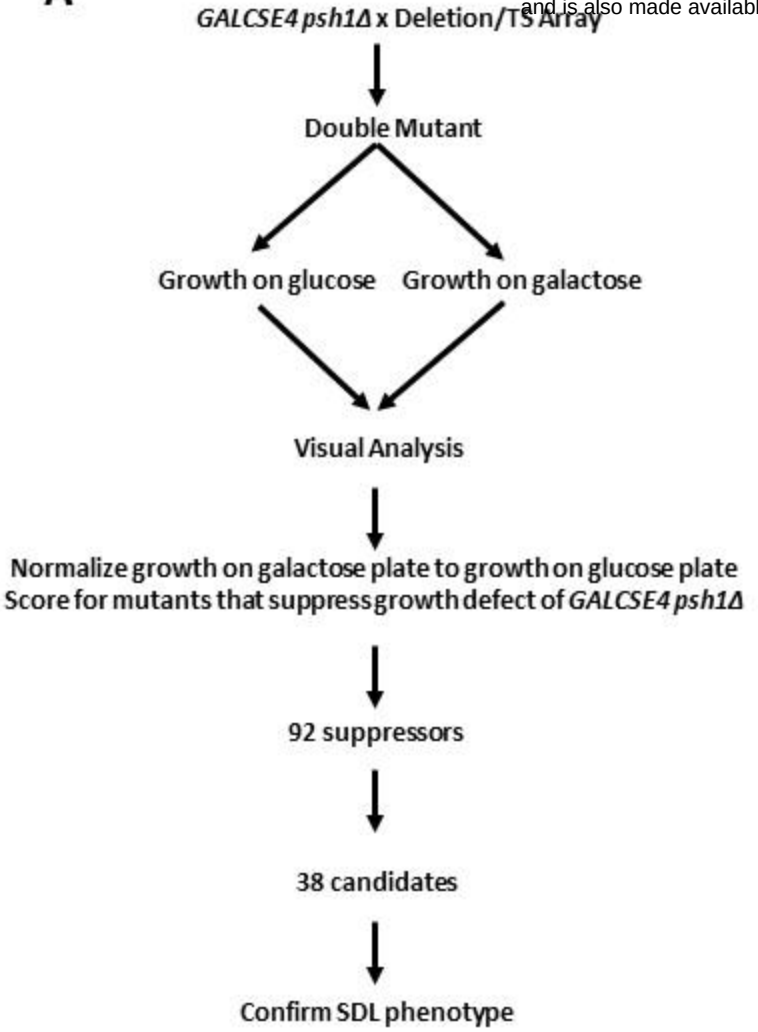

B

Figure 1

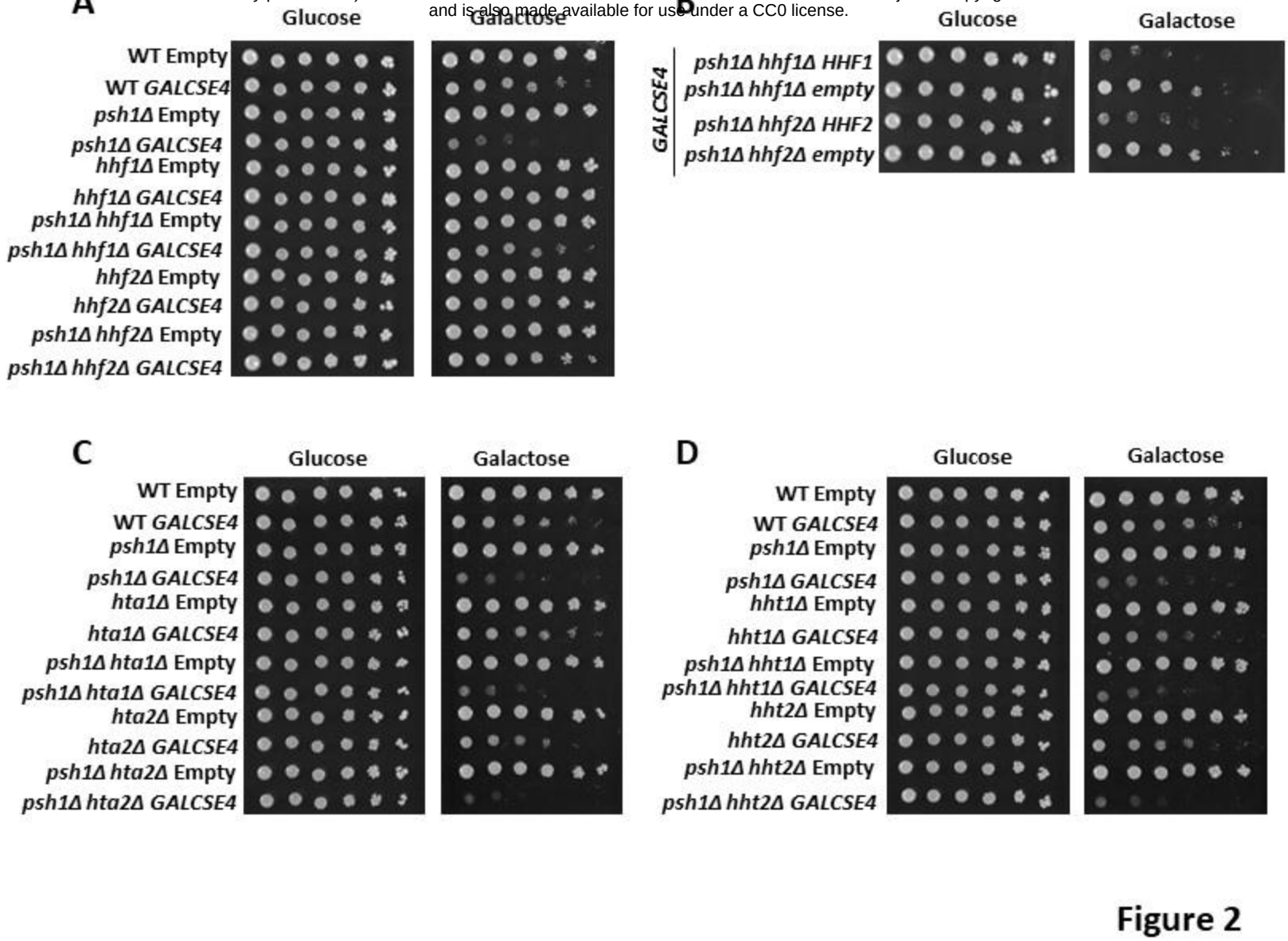

Figure 2

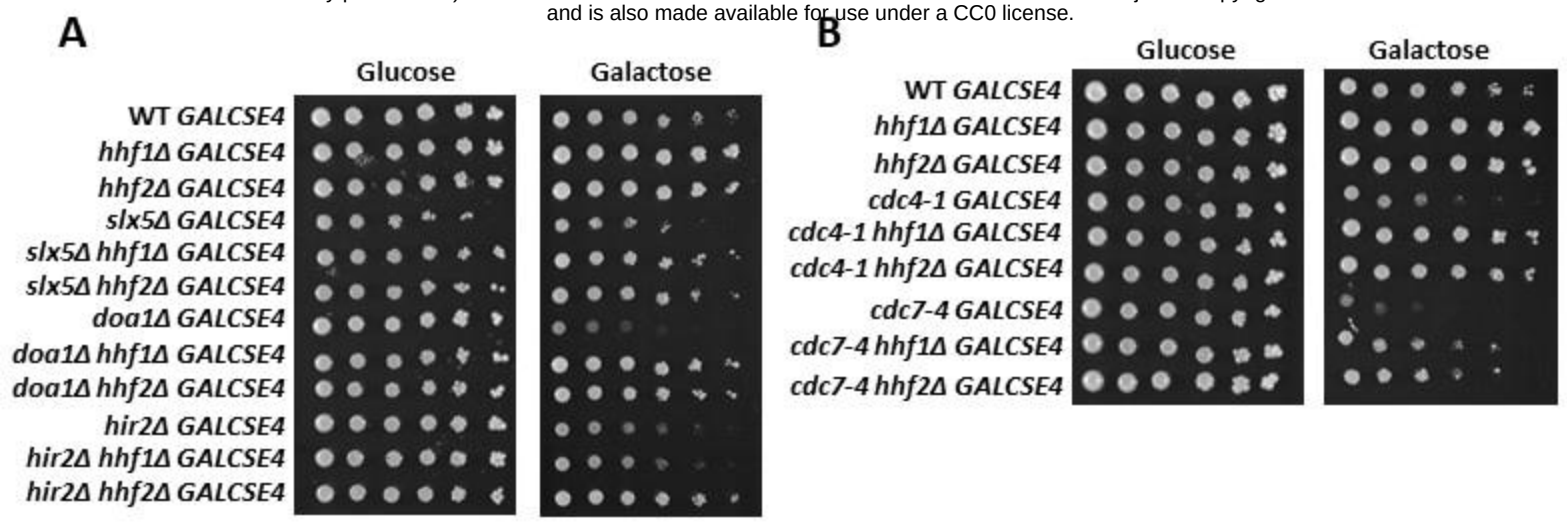

Figure 3

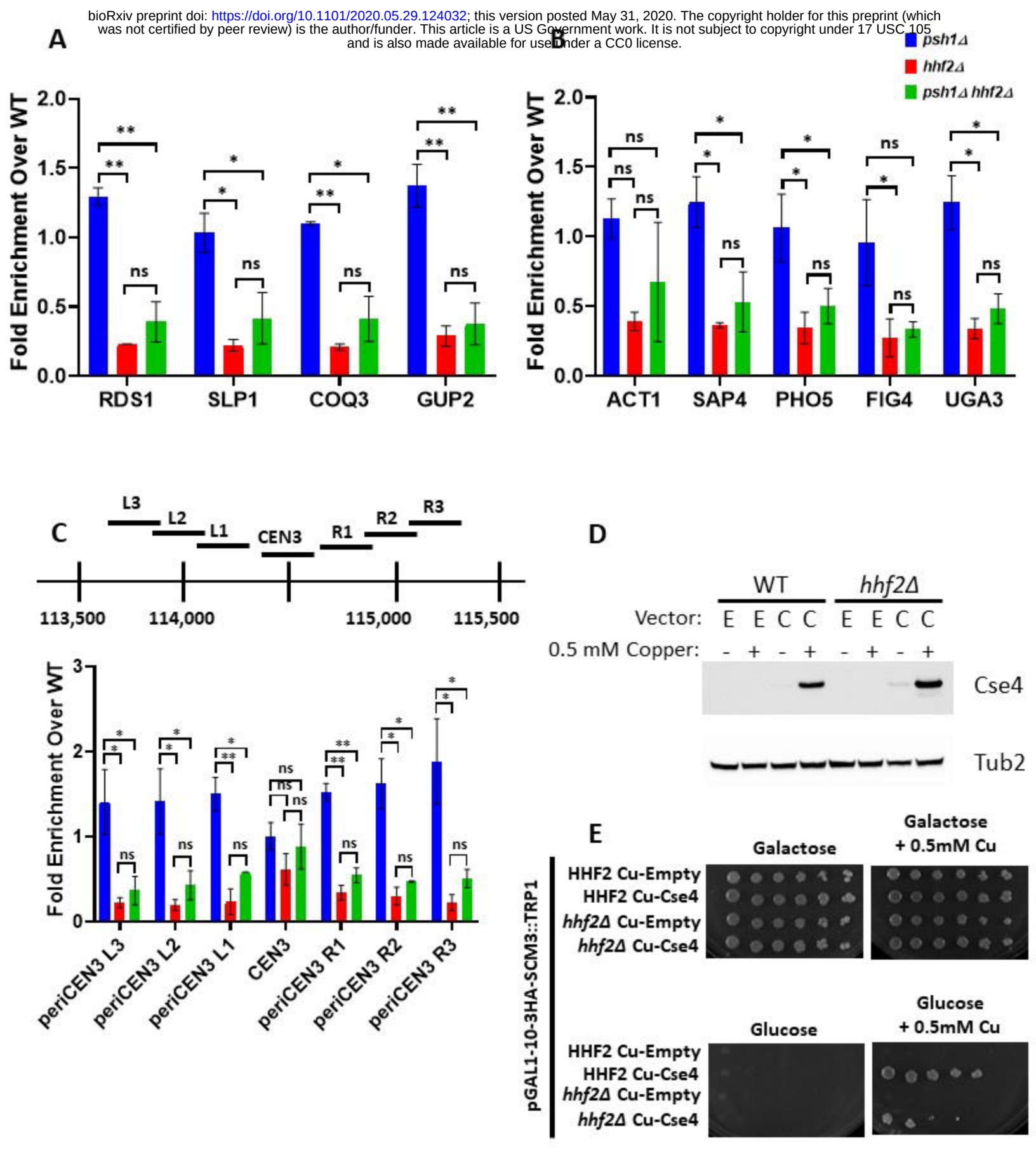

Figure 4

A

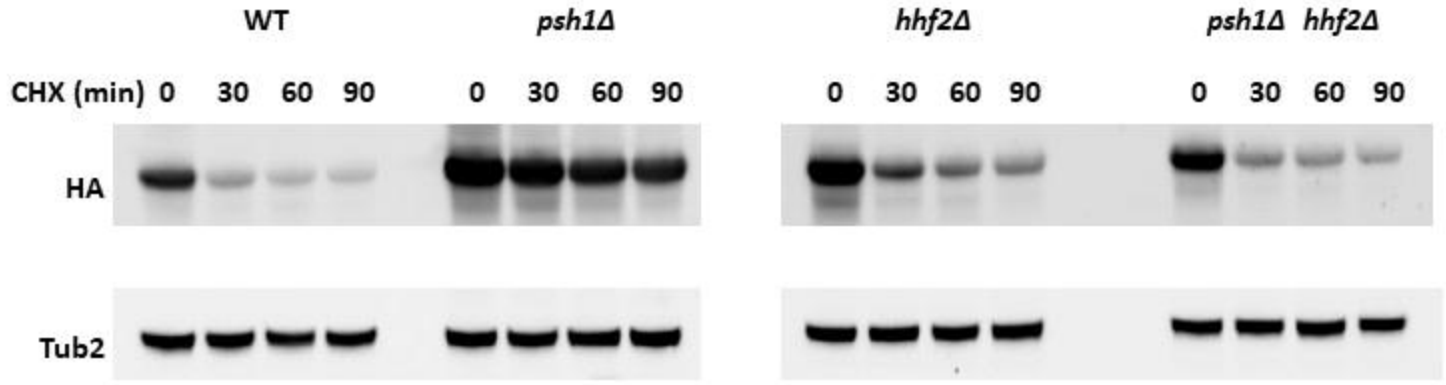

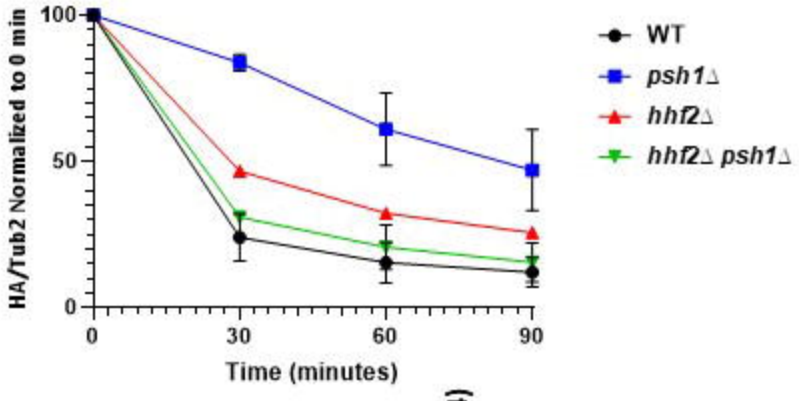

B

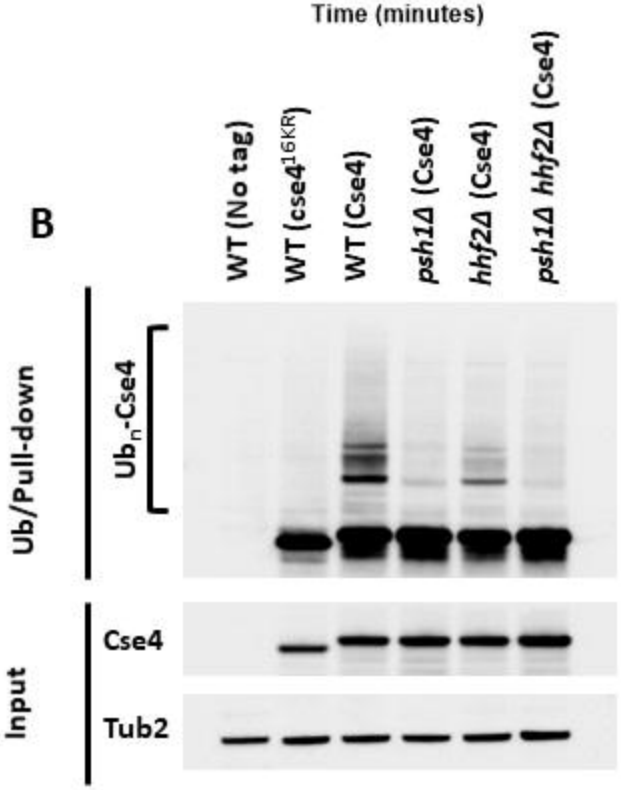

Strain	%Ub_n-Cse4
WT	100
cse4^{16KR}	20.8±2
psh1Δ	38.2±12.7
hhf2Δ	65.3±23.9
psh1Δ hhf2Δ	31.7±12.3

Figure 5

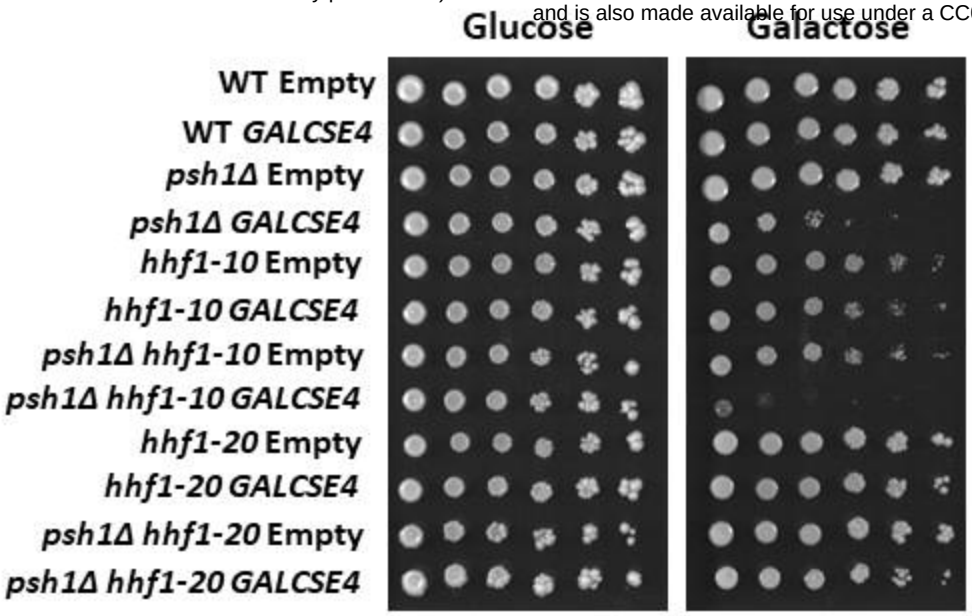

Figure 6